

ESD-TR-70-53

## ESD ACCESSION LIST

ESTI Call No.

69384

Copy No.

/ of /

cys.

Technical Note

1970-8

M. L. Rosenthal

VHF Antenna System  
for Aircraft

12 March 1970

Prepared under Electronic Systems Division Contract AF 19(628)-5167 by

Lincoln Laboratory

MASSACHUSETTS INSTITUTE OF TECHNOLOGY

Lexington, Massachusetts



ESD RECORD COPY

RETURN TO  
SCIENTIFIC & TECHNICAL INFORMATION DIVISION  
(ESTI), BUILDING 1211

AD705170

This document has been approved for public release and sale;  
its distribution is unlimited.

MASSACHUSETTS INSTITUTE OF TECHNOLOGY  
LINCOLN LABORATORY

VHF ANTENNA SYSTEM FOR AIRCRAFT

*M. L. ROSENTHAL*

*Group 61*

TECHNICAL NOTE 1970-8

12 MARCH 1970

This document has been approved for public release and sale;  
its distribution is unlimited.

LEXINGTON

MASSACHUSETTS

The work reported in this document was performed at Lincoln Laboratory, a center for research operated by Massachusetts Institute of Technology, with the support of the Department of the Air Force under Contract AF 19(628)-5167.

This report may be reproduced to satisfy needs of U.S. Government agencies.

## ABSTRACT

Presented are the initial results of a theoretical investigation of crossed-slot antenna elements arrayed on an aircraft to provide communications with satellites in the 225 to 400 MHz frequency range. Calculations indicate that two four-element array antennas can approximate the desired performance of covering the hemisphere above the aircraft with more than 6 dB directive gain. Including the polarization loss between the elliptically polarized aircraft antenna and the circularly polarized satellite antenna, coverage is provided over about 90 percent of the desired area.

Accepted for the Air Force  
Franklin C. Hudson  
Chief, Lincoln Laboratory Office

## CONTENTS

I.	Introduction	1
II.	Requirements	2
III.	General Description	3
IV.	Operation	3
V.	Performance	5
VI.	Modifications	32
VII.	Conclusion	37

## VHF Antenna System for Aircraft

### I. INTRODUCTION

Military aircraft require more effective antennas, operating in the 225 to 400 MHz frequency range, than are presently available. These antennas are often used for communicating with an artificial satellite which may be anywhere in the hemisphere, from the horizon to zenith above the aircraft. Therefore, the antenna should provide significantly more directive gain<sup>1</sup> than that of an isotropic radiator over this hemisphere. None of the presently employed antennas meet this requirement. A shallow-cavity crossed-slot antenna<sup>2</sup> has a directivity<sup>1</sup> of 4 to 6 dB; however, the directive gain is approximately that of an isotropic radiator over substantial portions of the desired area of coverage. To date, this crossed-slot antenna is about the best available for use on aircraft because of its directive gain, radiation efficiency, and shallow profile.

Initial results of a study show that crossed slots should be used as the radiating elements of an array antenna. The antenna system proposed here consists of two, four-element arrays mounted on the aircraft body. Beam steering permits the direction of the major lobe, of either array, to be toward the satellite for the transmission or reception of communications data. These major lobes are circularly polarized and provide at least 6 dB directivity over about 90 percent of the desired area of coverage.

## II. REQUIREMENTS

An arbitrary, but reasonable, ideal goal would be to cover the entire hemisphere above the aircraft with a minimum directive gain of 6 dB. Coverage should extend  $10^\circ$  below the horizon to provide communications when the craft banks for turns. However, ideally there should be no coverage below  $10^\circ$  to reduce the reception of noise from Earth. Circular polarization is required primarily because of the uncertainty of the relative orientation of linearly polarized antennas if they were used on the satellite and the aircraft. Other reasons for the use of circular polarization are the polarization uncertainties due to Faraday and multipath effects.

The antenna system must operate at two frequencies in the 225 to 400 MHz VHF band: one for transmitting and one for receiving. Initial work was based on the Sixth Lincoln Experimental Satellite (LES-6) which has a right-hand circularly polarized antenna system.<sup>3, 4</sup> Emphasis was placed on the satellite's higher (receive) frequency as it is the transmit frequency for the aircraft. Results at this frequency are applicable over the entire VHF band by scaling the key antenna dimensions.

Other requirements are that the antenna elements must have a low silhouette (they must not have an adverse aerodynamic effect) and the cost of producing, installing and operating the system must be low enough to make its use practical on both existing and future aircraft.



### III. GENERAL DESCRIPTION

Two array antennas are located on the airplane as shown in Fig. 1: one on the left and one on the right side. Between the center of each array and the top of the fuselage, the angle is about  $50^\circ$ . Each antenna consists of four crossed-slot elements arrayed as shown in the figure. Each element is circularly polarized.

Radio frequency energy passing through the transmission line to each element is adjusted to the desired phase relative to the other elements by variable phasing devices. Since only one array is used at a time, only one set of phasing devices is required. This set is switched between the two arrays by a four-pole double-throw radio-frequency switch as shown in Fig. 2. If variable phasing devices with a large enough range are available, a more economical arrangement may be to fix the phase of one element as the reference phase and only vary the phase of the other three. However, the saving due to the elimination of one phasing unit may be offset by the increase in cost of the other three which must have twice the range required by those in the system shown.

The array in use is connected through the phasing units to the transmitter and the receiver. Simultaneous transmission and reception of communications data is accomplished with a diplexer, as shown in the figure.

### IV. OPERATION

Successful operation of this system depends on prior knowledge of the

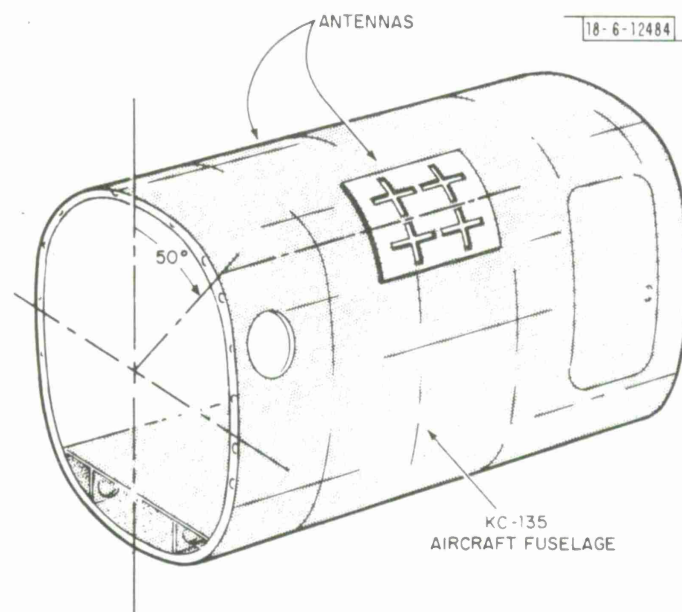


Fig. 1. Array of four crossed slots on each side of aircraft.

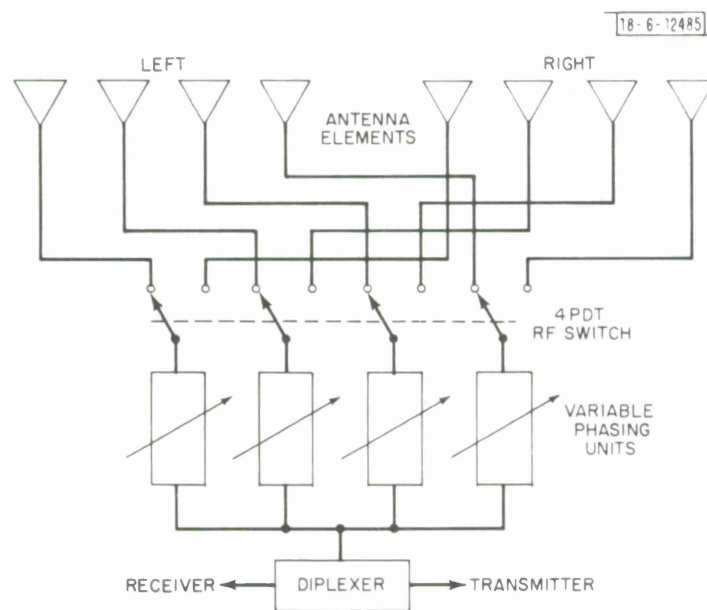


Fig. 2. Basic system block diagram.

location and availability of the satellite through which the aircraft will communicate. In the general case, the satellite will be randomly located and the appropriate array antenna is selected by connecting it to the phasing units with the 4PDT RF switch. The phasing devices are then adjusted to form that beam which points to the satellite. This could provide the largest possible antenna directivity at both frequencies. However, because beam pointing is a function of frequency, the phase will most likely have to be a compromise between the best values for transmitting and receiving.

Additionally, an economical design may require that the phase be varied in steps, rather than continuously. This would also be a factor in obtaining the maximum gain in the direction of the satellite.

However, all these factors, including the satellite-location information, could be put into the system for either automatic or operator-controlled operation. In the automatic mode of operation, the operator would only have to know the pointing angles between the aircraft and the satellite. This information would be fed into a control unit and the switching and phasing would be accomplished automatically in accordance with a pre-programmed procedure. This procedure could also provide for optimizing the phasing for both the transmit and receive frequencies.

## V. PERFORMANCE

Calculated results indicate that a 6 dB minimum directive gain can be obtained over about 90 percent of the upper hemisphere plus about  $10^\circ$  below

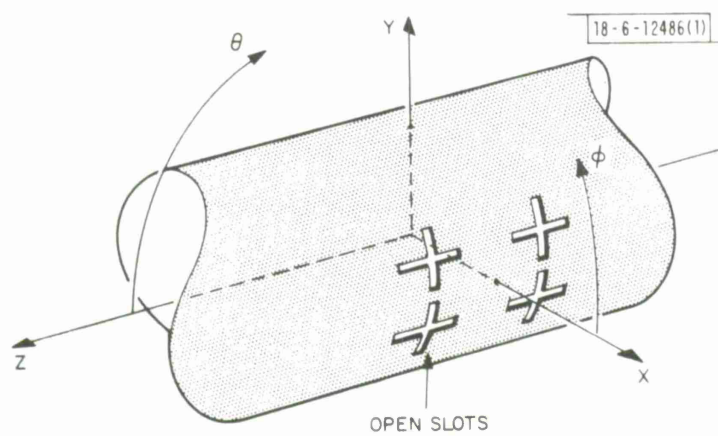


Fig. 3. Crossed-slot array on infinitely long cylinder in spherical coordinate system.

the horizon. Over 80 percent of that same region of coverage, the axial ratio is less than 6 dB. For those cases where the maximum of the beam can point directly at the satellite, the directivity will be about 11 dB at the transmit frequency.

Theoretical directive gain and axial ratios are based on a program which computes the radiation characteristics of slot antenna elements on the surface of a cylinder.<sup>5</sup> For arrays of identical rows of either axial or circumferential slots on infinitely long cylinders, this program gives the relative magnitude and phase of the far field (at any point in space) as well as the directive gain relative to a linearly polarized isotropic radiator. An additional program combines the orthogonal linearly polarized fields from sets of axial and circumferential slots and describes the resulting elliptically polarized fields in terms of the axial ratio, sense of polarization and directivity to matched polarization.

Figure 3 shows arrays of axial and circumferential slots on the surface of an infinitely long conducting cylinder in the spherical coordinate system used to compute and present the radiation characteristics. The cylinder is shown in the conventional right-hand coordinate system and it should be recognized as representing the fuselage of the aircraft. Therefore, the directions of the nose and tail correspond to  $\theta = 0^\circ$  and  $\theta = 180^\circ$ , respectively. An array of two rows of two axial slots per row and a similar array of circumferential slots form the four crossed-slot array described previously.

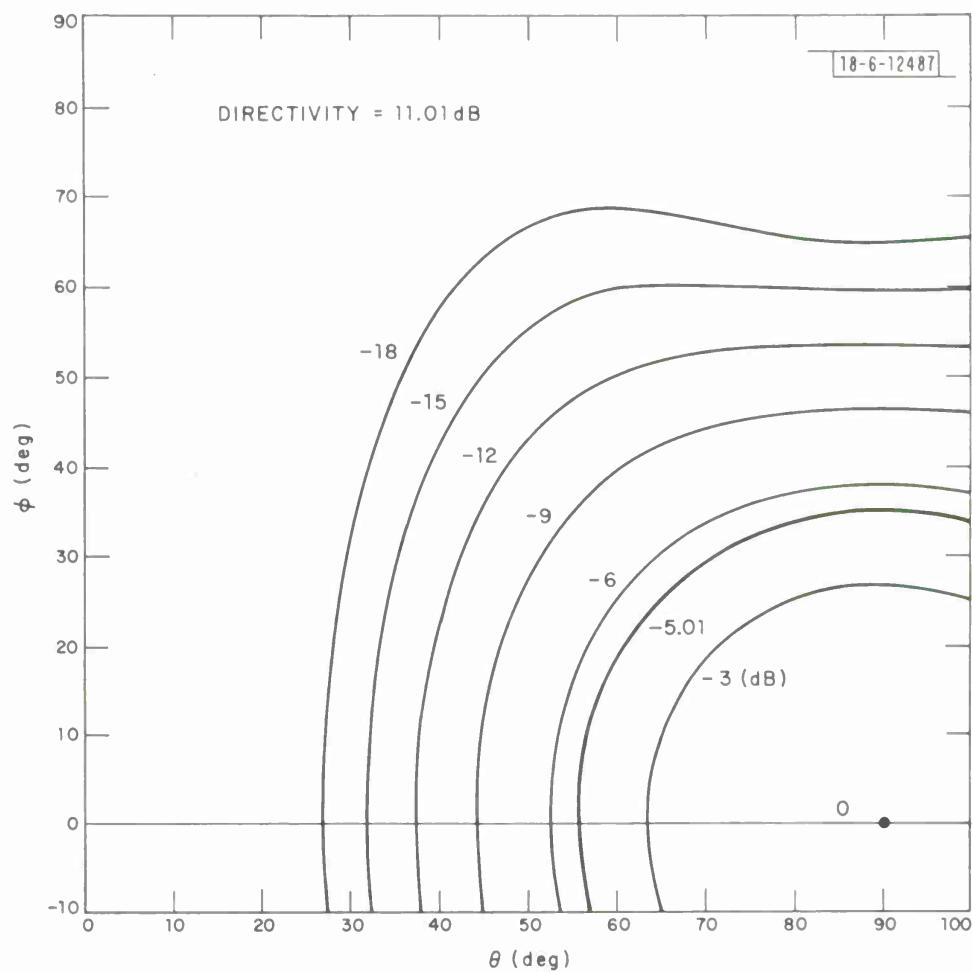


Fig. 4. Directive-gain contours of 2 x 2 array of in-phase crossed slots  $\lambda/2$  long,  $\lambda/2$  apart on  $1.87\lambda$  radius cylinder. Maximum directivity = 11.01 dB.

The center of this array is at  $\theta = 90^\circ$ ,  $\phi = 0^\circ$ . If the axial slots are fed in phase quadrature with the circumferential slots and with equal magnitude of the excitation voltage for all slots, the maximum field strength will occur at  $\theta = 90^\circ$ ,  $\phi = 0^\circ$  where the polarization will be circular. Figure 4 is a contour plot of the directive gain of this configuration. All slots are one-half wavelength ( $\lambda/2$ ) long and are spaced  $\lambda/2$  apart (measured between centers) on a cylinder of  $1.87\lambda$  radius. This latter dimension approximates the fuselage of a KC-135 aircraft at the transmit frequency.

Contours in this and the following figures are plotted relative to the antenna directivity (11.01 dB in this case) in 3 dB steps (so that the first contour is labeled "-3" and the second "-6", etc., down to -18 dB) with the exception of the accented contour which represents 6 dB directive gain. All values of directivity and directive gain are relative to that of an isotropic radiator of matched polarization. That is, at each point in space, the gain is compared to that of an isotropic antenna with the same polarization characteristics: the same sense, axial ratio and orientation of the polarization ellipse.

The field equations, referred to previously,<sup>5</sup> give the amplitude and phase of the far field produced by the axial and circumferential slots for a specified voltage excitation at the center of each slot. For this initial analysis, power is considered to be equally divided between the axial and the circumferential arrays. This does not necessarily produce orthogonal fields of

equal amplitude, but it is a reasonable approximation of this condition. The directivity is used to adjust the field strength produced by the axial and circumferential slot arrays. Using functional notation, the axial-slot field vector which is polarized in the  $\phi$ -direction can be defined by

$$\vec{E}_{\phi}(\theta, \phi) = \vec{\mu}_{\phi} E_a(\theta, \phi) e^{j\beta_a(\theta, \phi)} \quad (1)$$

where  $\vec{\mu}_{\phi}$  is a unit vector pointing in the positive  $\phi$ -direction,  $E_a$  is the magnitude of the axial-slot field and  $\beta_a$  is the phase. Similarly, the circumferential-slot field vector is defined by

$$\vec{E}_{\theta}(\theta, \phi) = \vec{\mu}_{\theta} E_c(\theta, \phi) e^{j[\beta_c(\theta, \phi) + \Delta]} \quad (2)$$

where  $\vec{\mu}_{\theta}$  is a unit vector pointing in the positive  $\theta$ -direction,  $E_c$  is the magnitude of the circumferential-slot field and  $\beta_c$  is the phase.  $\Delta$  adjusts the phase between the two orthogonal fields. At each point, the phase difference between  $\vec{E}_{\theta}$  and  $\vec{E}_{\phi}$  is

$$\delta = \beta_c + \Delta - \beta_a \quad (3)$$

Usually, the attempt will be made to have  $\delta = \pm 90^\circ$  for low axial ratios over as much of the beam as possible.

The power radiated in either field can be shown to be given by

$$P_r = 4\pi r^2 E^2 / \eta \quad (4)$$



where  $E$  is either  $E_a$  or  $E_c$  and  $\eta$  is the intrinsic impedance of free space.

The directive gain for either field is the ratio of the power radiated to the input power, or

$$D = \frac{P_r}{P_i} = \frac{4\pi r^2 E^2}{\eta P_i} = KE^2 \quad (5)$$

Since  $P_i$  is a constant (equal power into each array, axial and circumferential) it can be included in  $K$  along with the other constants. From Eq. (5) it follows

$$\frac{E_a}{E_c} = \sqrt{\frac{D_a}{D_c}} \quad (6)$$

where  $D_a$  and  $D_c$  are the directive gains for the axial and circumferential slot arrays, respectively.  $D_a$  and  $D_c$  are computed as functions of  $\theta$  and  $\phi$  by the program referred to previously.<sup>5</sup>

The directive gain to matched polarization is given by

$$D_m = \frac{4\pi r^2 (\vec{E}_\phi + \vec{E}_\theta) \cdot (\vec{E}_\phi + \vec{E}_\theta)^*}{\eta(P_{ia} + P_{ic})} \quad (7)$$

$$= \frac{1}{2} (D_a + D_c)$$

where the asterisk indicates the complex conjugate of  $\vec{E}$ ;  $P_{ia}$  and  $P_{ic}$  are the input power to the axial and circumferential slot arrays. In the present case

$$P_{ia} = P_{ic}.$$

From the foregoing, all the desired characteristics of the radiated field can be computed as a function of  $\theta$  and  $\phi$  and plotted as contours in the  $\theta, \phi$  plane. The directive gain to matched polarization is given in dB by

$$D_m = 10 \log \frac{1}{2} (D_a + D_c) \quad (8)$$

The polarization ellipse tilt angle is

$$\tau = \frac{1}{2} \arctan \frac{2(E_a/E_c) \cos \delta}{(E_a/E_c)^2 - 1} \quad (9)$$

where  $E_a/E_c$  is given by Eq. (6). The sense and the axial ratio are given by

$$r = \pm \left| 10 \log \frac{\cos^2(\tau + \frac{\pi}{2}) - (E_a/E_c) \cos \delta \sin 2(\tau + \frac{\pi}{2}) + (E_a/E_c)^2 \sin^2(\tau + \frac{\pi}{2})}{\cos^2 \tau - (E_a/E_c) \cos \delta \sin 2\tau + (E_a/E_c)^2 \sin^2 \tau} \right| \text{dB} \quad (10)$$

If  $0 < \delta < 180^\circ$ ,  $r$  is + for left-hand sense;

if  $-180^\circ < \delta < 0$ ,  $r$  is - for right-hand sense.

Figure 4 is a plot of Eq. (8) for the case described, with  $\Delta = 90^\circ$ . Thus,  $\theta = 90^\circ$ ,  $\phi = 0^\circ$  is the normal direction of the array antenna and this is where the maximum field strength occurs. Note that advantage is taken of symmetry so that only one-quarter of the region need be presented. Actually  $\theta$  is

extended to  $100^\circ$  and  $\phi$  to  $-10^\circ$  to show the contours in the first ten degrees of the adjacent quadrants.

Figure 5 is a plot of Eq. (10) for the same case. Contours of axial ratio are plotted in 1 dB steps. At  $(90^\circ, 0^\circ)$  the field is circularly polarized so the axial ratio is low; the first contour is 1 dB, the second 2 dB, etc., up to a maximum of 9 dB. Over the region shown, all the values are positive, therefore the sense is left hand. Changing to right-hand sense, is easily accomplished by reversing the sign of  $\Delta$ , as can be seen from Eqs. (3) and (10). High axial ratios and/or reversal of sense within the region of  $> 6$  dB gain are of major significance. Superimposing Figs. 4 and 5 shows that for the region enclosed by the -5.01 dB relative directive gain contour (the  $> 6$  dB directive gain region) axial ratios are less than 3 dB; in fact, over most of the region they are  $< 2$  dB.

If a phase difference is introduced between the upper and lower rows of slots, of Fig. 3, the beam will be tilted in the  $\phi$ -direction. Similarly, a phase difference between the left and right columns will tilt the beam in the  $\theta$ -direction. Figure 6 shows the results of a  $60^\circ$  phase difference between rows and a  $120^\circ$  phase difference between columns. Maximum gain of 9.50 dB occurs at the point  $(60^\circ, 15^\circ)$ . Figure 7 shows the corresponding axial ratio plot. Now the  $> 6$  dB gain region (enclosed by the -3.50 dB contour) has been shifted up and to the left. This has been accompanied by a deterioration in axial ratio to a maximum of about 7 dB. However, no attempt was made to

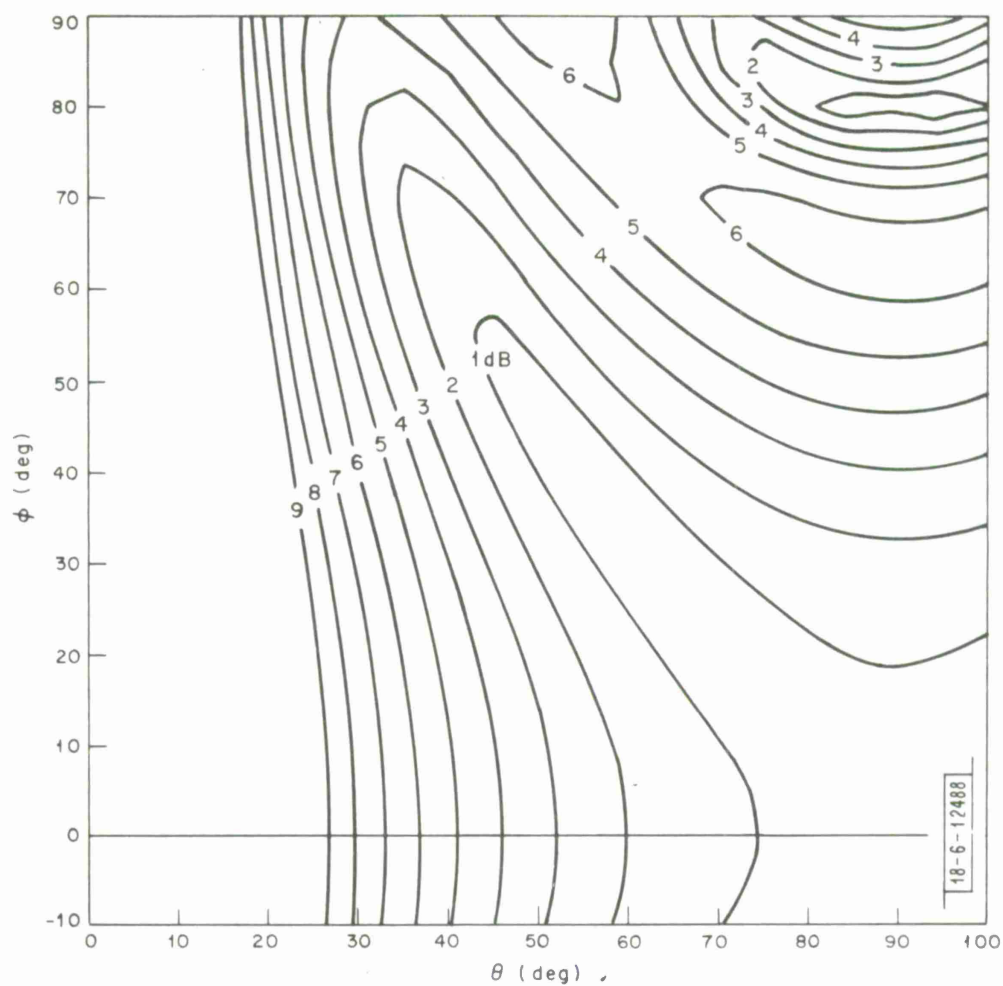


Fig. 5. Axial-ratio contours for array of Fig. 4.

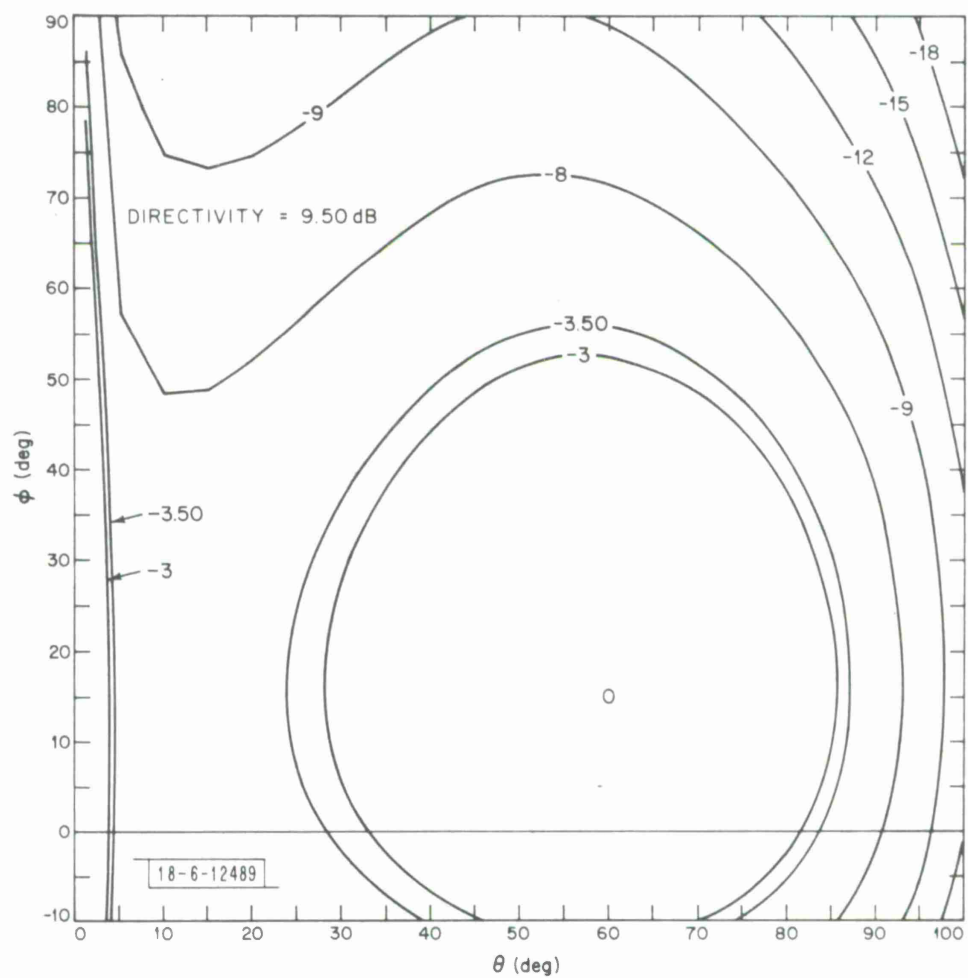


Fig. 6. Directive-gain contours for array of Fig. 4, but with  $120^\circ$  phase difference between columns and  $60^\circ$  difference between rows.

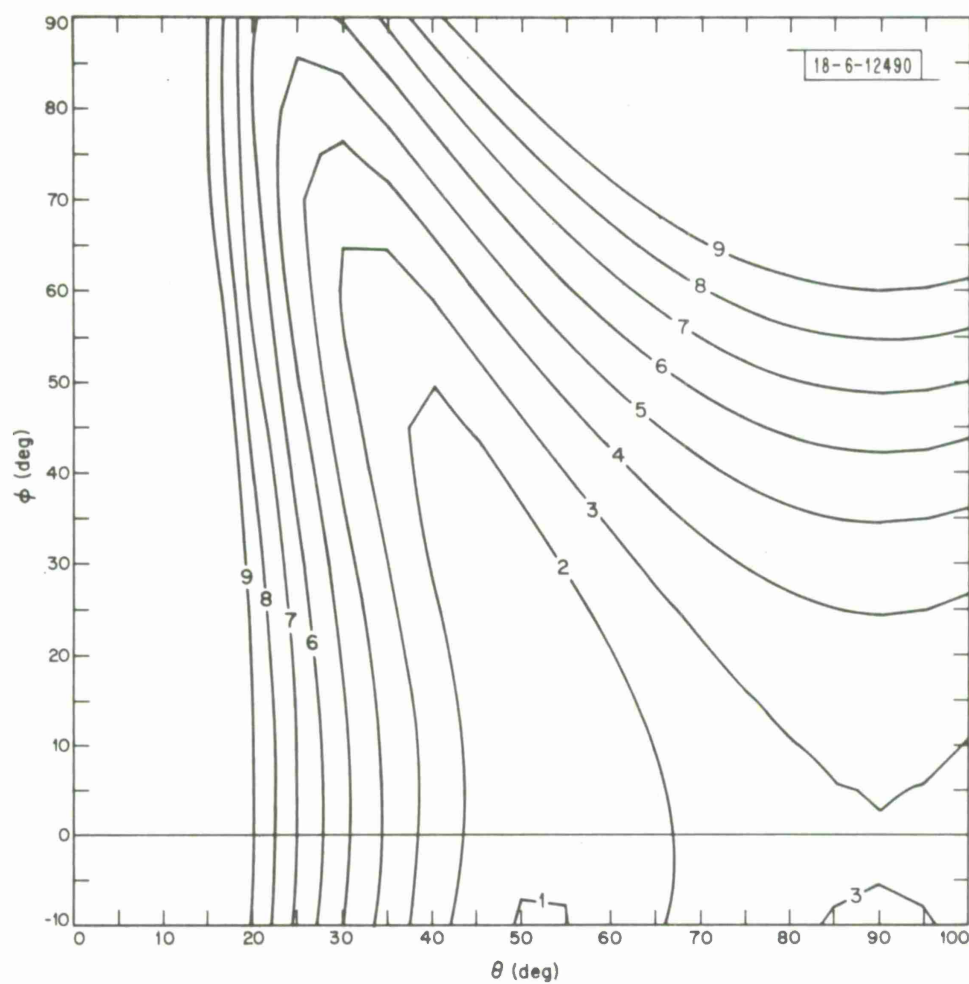


Fig. 7. Axial-ratio contours for array of Fig. 6.

optimize the axial ratios over the  $> 6$  dB gain region; that is,  $\Delta$  was not changed to improve the overall axial ratio.

Equations (3), (9) and (10) show that the axial ratio is minimum when  $\delta = 90^\circ$ , and this can only occur when  $\beta_a = \beta_c$  if  $\Delta = 90^\circ$ . With the same excitation for both the axial and circumferential slot arrays, the values of  $\beta_a$  and  $\beta_c$  are close enough to each other at corresponding points in space for  $60^\circ < \delta < 120^\circ$  over the region of interest. Therefore, the magnitudes of the two fields are a more important factor than the phases in determining the axial ratio. In view of this,  $\Delta$  was made an independent parameter  $= 90^\circ$ .

Figures 4 through 7 are plots representing two of 16 cases which were computed and plotted for  $\lambda/2$  slots,  $\lambda/2$  apart. These 16 cases were a systematic investigation of the effect of changing the excitation phase between both rows and columns from  $0^\circ$  through  $180^\circ$  in  $60^\circ$  steps. Excitation voltage magnitudes were all equal, only the phase was changed.

Figure 8 is a composite plot of the maximum directive gain at each point  $(\theta, \phi)$  for the 16 cases. Thus it represents the best coverage that can be obtained when the phase adjustment is limited to discrete steps of  $60^\circ$  each. Naturally, the maximum gain of the region shown is 11.01 dB at the point  $(90^\circ, 0^\circ)$  provided by the in-phase case of Fig. 4. However, the in-phase case has a half-power beamwidth of only about  $54^\circ$ , as indicated by the  $\sim 27^\circ$  radius of the -3 dB contour on Fig. 4, whereas the composite has a "HPBW"  $> 100^\circ$  as indicated by the  $> 50^\circ$  radius of the -3 dB contour on Fig. 8.

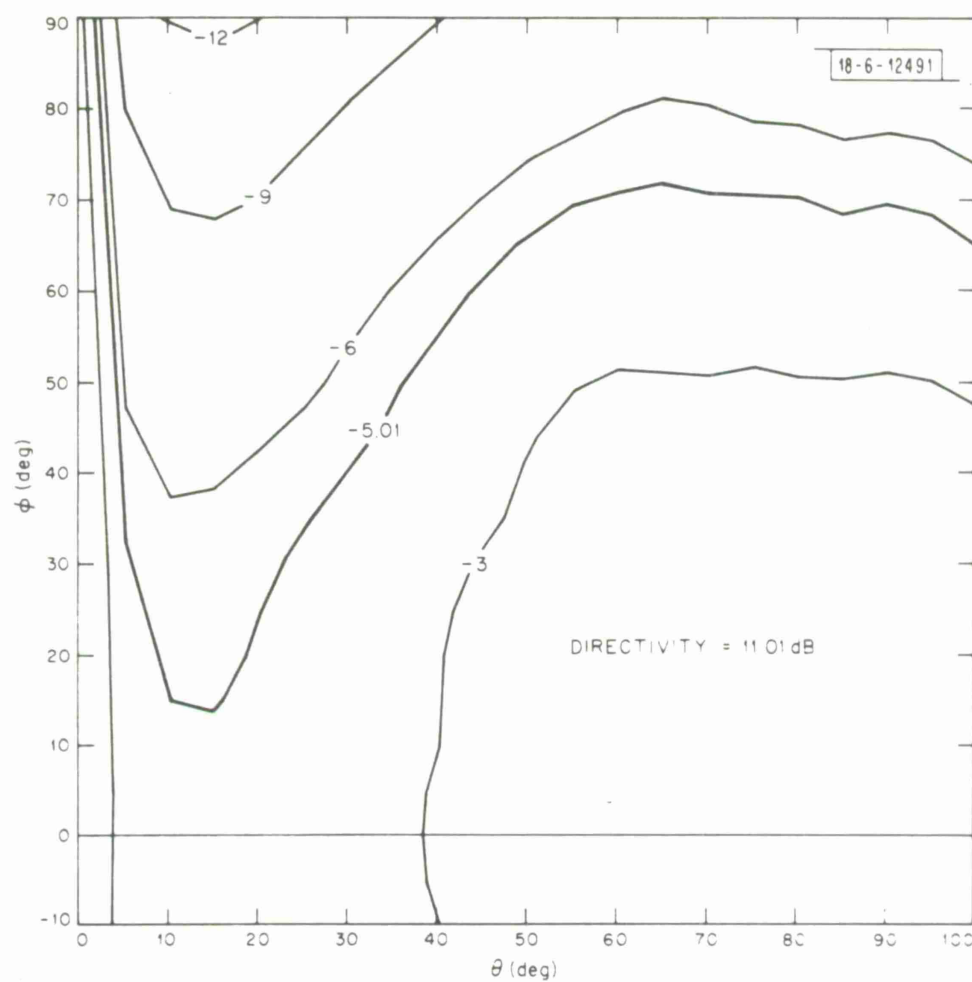


Fig. 8. Composite of maximum directive-gain contours for array of Fig. 4 with phase varied in both directions from  $0^\circ$  to  $180^\circ$  in  $60^\circ$  steps (16 cases). Maximum directivity = 11.01 dB.



As before, coverage in the other three quadrants is given by symmetry because the phase relationships between either the rows or the columns (or both) can be interchanged. Again, the level of 6 dB over isotropic is accented.

Figure 9 is the composite plot of the axial ratio corresponding to the maximum directive gain at each point. Using symmetry, the axial ratio is  $< 6$  dB for the region bounded as follows:

$$23^\circ < \theta < 157^\circ \text{ and } -63^\circ < \phi < +63^\circ .$$

For  $\theta < 23^\circ$  or  $\theta > 157^\circ$  the axial ratio increases rapidly as the axis of the cylinder is approached. At  $\theta = 0^\circ$  or  $180^\circ$  the tangential field vanishes and only a linearly polarized field can exist. Thus, the axial-slot field strength falls rapidly as  $\theta$  approaches zero or  $180^\circ$ .

In the  $\phi$  plane, coverage is better than needed. If the array were located on the side of the aircraft  $63^\circ$  down from the top, the axial ratio would be less than 6 dB from zenith to  $2(63^\circ) - 90^\circ = 36^\circ$  below the horizon. As indicated by Fig. 1, the array would be placed  $50^\circ$  down from the top to provide coverage from zenith to  $2(50^\circ) - 90^\circ = 10^\circ$  below the horizon. Therefore, the ideal area on the surface of a sphere would be that of a lune bounded by:

$$0 < \theta < 180^\circ \text{ and } -50^\circ < \phi < +50^\circ .$$

Figure 10 is a repeat of Fig. 8 with an overlay of dashed curves showing the ideal area of coverage divided into smaller areas bounded by curves

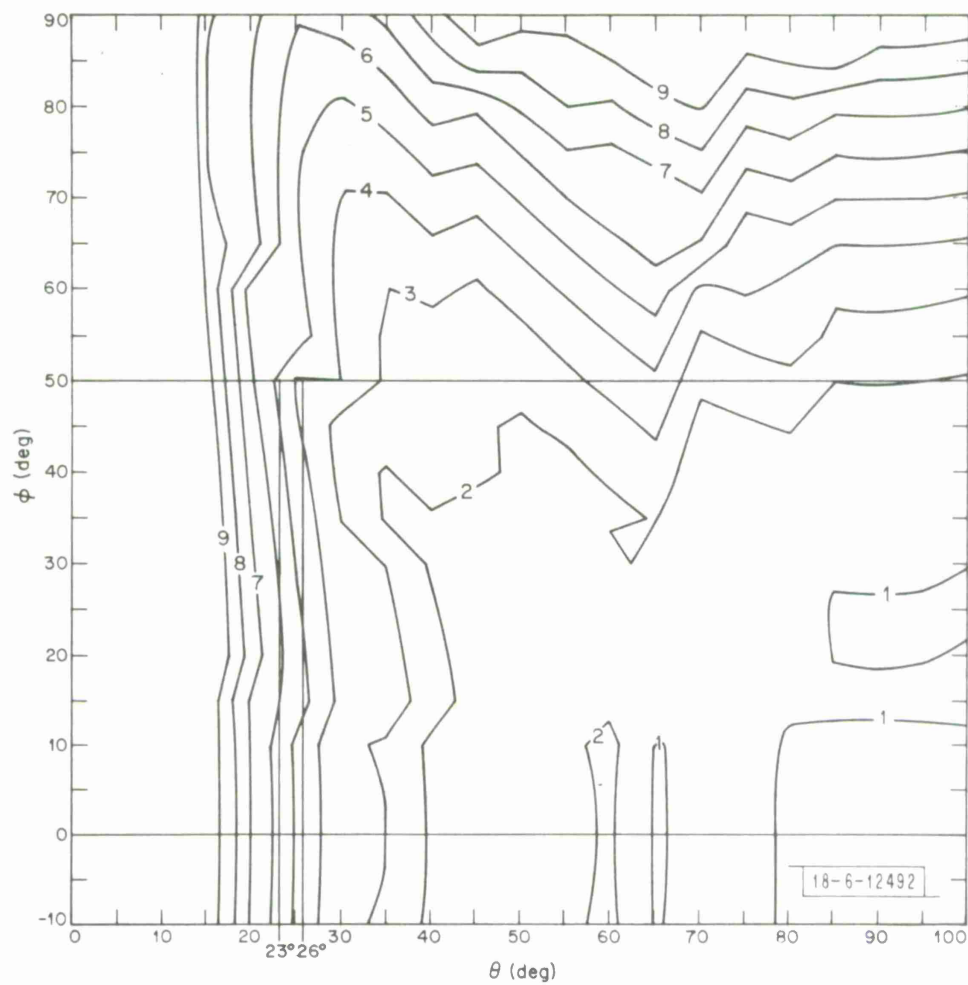


Fig. 9. Contours of axial ratios related to maximum directive gains for array of Fig. 8.

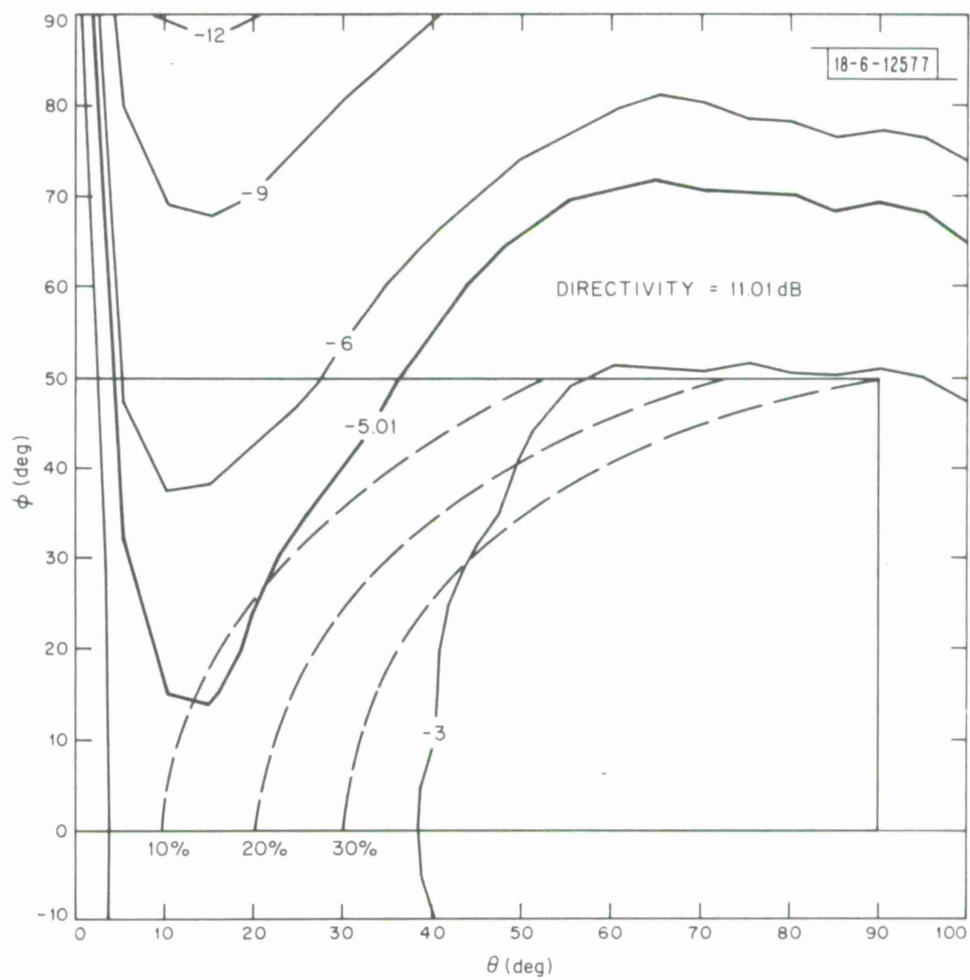


Fig. 10. Composite directive-gain contours of Fig. 8 with overlay showing coverage areas.

approximating the contours so that the amount of coverage can be readily estimated. Again, only one quarter of the area is shown, the rest being inferred by symmetry. Therefore, the rectangular area outlined on the overlay represents that portion of the surface of a sphere bounded by  $0 < \theta < 90^\circ$  and  $0 < \phi < 50^\circ$  (a spherical triangle  $50^\circ \times 90^\circ \times 90^\circ$ ). Since the entire area of a unit sphere is  $4\pi$ , the area shown is  $\pi/3.6$ .

Lines on the surface of the sphere are described by

$$\sin \theta = A - B \cos \phi$$

where the constants A and B are chosen to make curves approximating the directive gain contours. Then, the normalized area ( $A_o$ ) between  $\theta = 0$  and the curve is given by

$$A_o = \frac{3.6}{\pi} \int_0^{\pi/3.6} \int_0^\alpha \sin \theta \, d\theta \, d\phi \quad (11)$$

where  $\alpha = \arcsin (A - B \cos \phi)$ .

This expression was numerically integrated and the result expressed as a percent of the whole area ( $\pi/3.6$ ). Proper choice of constants A and B results in the dashed curves shown. With  $A = 1.9$  and  $B = 1.7264$ , the area is 10 percent. It is bounded by the left curve, of Fig. 10, which starts at the point  $(10^\circ, 0^\circ)$  and curves up to  $(52.2^\circ, 50^\circ)$  approximating the shape of the directive gain contours. For the 20 percent curve, which starts at

(20°, 0°),  $A = 2.05$  and  $B = 1.708$ ; while for the 30 percent curve,  $A = 1.905$  and  $B = 1.405$ .

Analysis of Fig. 10 shows that the -5.01 dB contour corresponds most nearly to the 10 percent area curve. In fact, the contour line encloses much more than 90 percent of the desired area of coverage; therefore, the directive gain exceeds 6 dB over this area. Similarly, comparison of the -3 dB contour with the 30 percent curve shows that the gain exceeds 8 dB over about 70 percent of the desired area.

For the axial ratio contours, such as shown in Fig. 9, a good approximation appears to be a line of constant  $\phi$  at the top of the plot and a line of constant  $\theta$  at the left side. A limit to the constant value of  $\phi$  has already been set:  $\phi = 50^\circ$ . Therefore, constant values can be chosen for  $\theta$  to divide the area of coverage into smaller areas as before. This is a relatively simple case and the integral can be solved analytically. Thus,

$$A'_0 = \frac{3.6}{\pi} \int_0^{\pi/3.6} \int_0^{\theta_1} \sin \theta \, d\theta \, d\phi = 1 - \cos \theta_1 \quad (12)$$

is the normalized area between  $\theta = 0$  and  $\theta = \theta_1$ .

Solving Eq. (12) for a relative area of 10 percent,  $\theta_1 = 26^\circ$ . This is shown in Fig. 9 and the 90 percent area bounded by  $26^\circ < \theta < 90^\circ$  and  $0^\circ < \phi < 50^\circ$  includes no part of the contour with axial ratio greater than 5 dB. Alternatively, assuming an axial-ratio limit of 6 dB would reduce  $\theta_1$  to about

23° which corresponds to an area of about 8 percent.

Therefore, two array antennas located as described previously in Fig. 1, would give satisfactory performance over more than 90 percent of the desired coverage area. However, shallow-cavity half-wave slots are frequency-sensitive high impedance elements and matching to the usually employed 50-ohm characteristic impedance transmission lines at two frequencies would be difficult. Crossed-slot aircraft antenna elements which have been built and tested<sup>2</sup> show a reasonable match when the slot length is about  $0.75\lambda$ .

The effect of increasing slot length had already been determined, before the impedance question was considered, when the results of a 20 percent increase in frequency was investigated. This results in slots  $0.6\lambda$  long and  $0.6\lambda$  apart on a  $2.24\lambda$  radius cylinder. Figures 11 and 12 are the composite gain and axial ratio plots, respectively, resulting from 25 cases computed for the  $0.6\lambda$  slot with the excitation phase between both rows and columns varied from  $0^\circ$  through  $180^\circ$  in  $60^\circ$  steps plus  $216^\circ$  to include the end-fire cases. Increasing the slot length and the separation between them beyond  $\lambda/2$  to  $0.6\lambda$  increases the maximum gain to 12.36 dB. It also results in the formation of grating lobes. However, the gain is still  $> 6$  dB over the more than 90 percent of the desired coverage area as shown by the -6.36 dB contour curve and the theoretical curve bounding the 10 percent area. Also, the axial ratio is  $< 6$  dB over the region bounded by  $26^\circ < \theta < 90^\circ$  and  $0^\circ < \phi < 50^\circ$  which encloses 90 percent of the desired area.

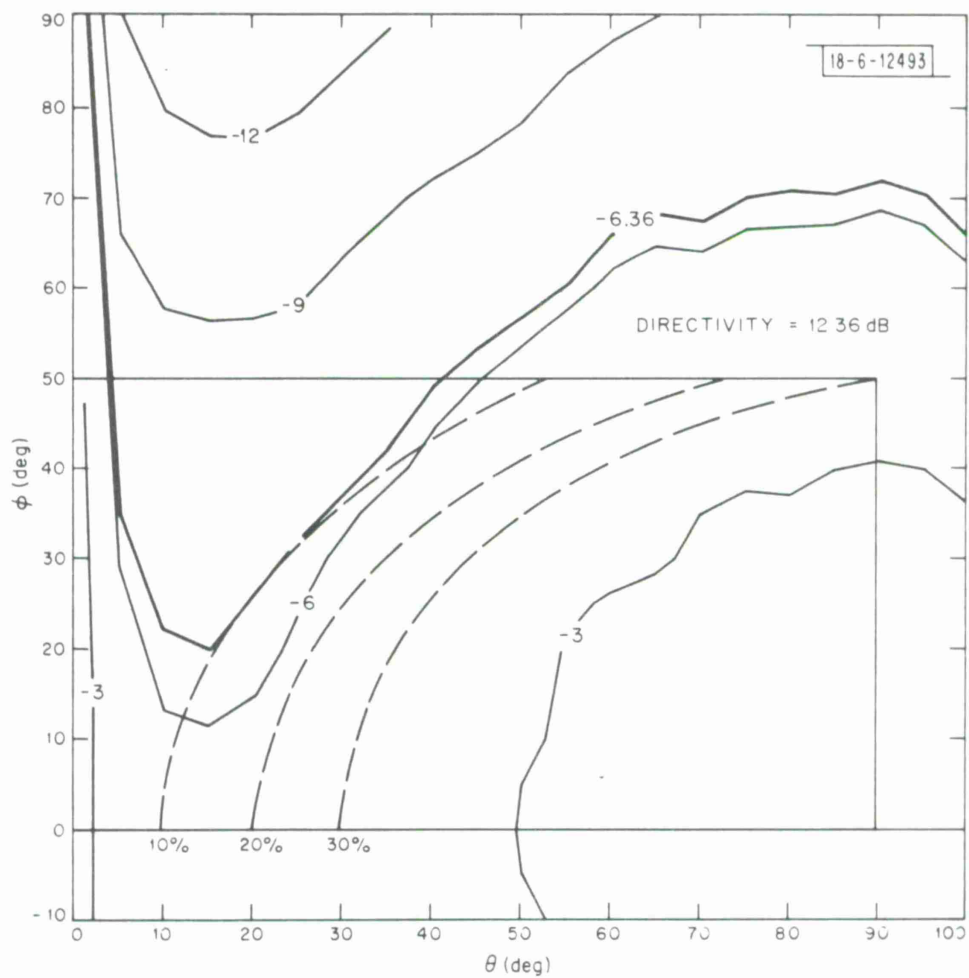


Fig. 11. Like Fig. 10, but for slots  $0.6\lambda$  long and  $0.6\lambda$  apart on  $2.24\lambda$  radius cylinder. Maximum directivity = 12.36 dB.

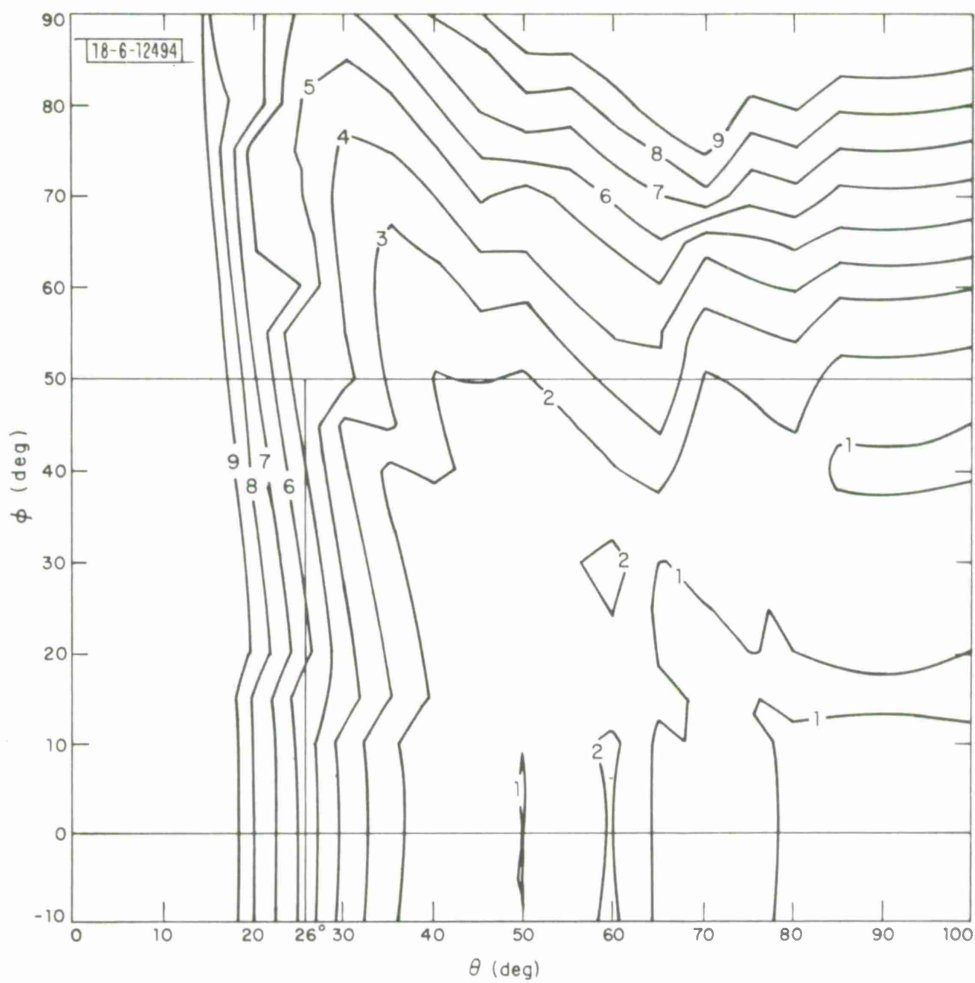


Fig. 12. Contours of axial ratios related to maximum directive gains for array of Fig. 11.



A 50 percent increase in frequency was also investigated resulting in slots  $0.75\lambda$  long and  $0.75\lambda$  apart on a  $2.8\lambda$  radius cylinder. Computed were 36 cases with excitation phase varied from  $0^\circ$  through  $240^\circ$  in  $60^\circ$  steps plus  $270^\circ$  for the end-fire cases. Figures 13 and 14 show the results. The maximum gain, 12.37 dB is practically the same as for the  $0.6\lambda$  case; and the gain coverage area is still about 90 percent of the desired area. However, the axial ratios have deteriorated so that they are  $< 6$  dB only over the region bounded by  $34^\circ < \theta < 90^\circ$  and  $0^\circ < \phi < 50^\circ$  which represents about 83 percent of the desired area of coverage. More work remains to be done to improve both the gain and the polarization characteristics in the forward and aft directions. This would most likely require modifications to the basic two-array system. Before going into such changes or additions, Fig. 15 is presented to make clear what the problem areas are. Shown is a view looking down on the aircraft from zenith. Contours of modified directive gain for the entire area of coverage are plotted in one dB steps. Accented is the 6 dB contour.

Modified directive gain includes the polarization loss due to the elliptical polarization of the aircraft antenna, assuming the satellite antenna to be perfectly circularly polarized. For axial ratios less than 6 dB, the polarization loss is less than  $1/2$  dB. Therefore, over most of the area of coverage, this loss can be neglected. However, in the fore and aft regions (where the aircraft antenna is virtually linearly polarized) the polarization loss approaches 3 dB. In these regions the directive gain is below the 6 dB goal, as can be

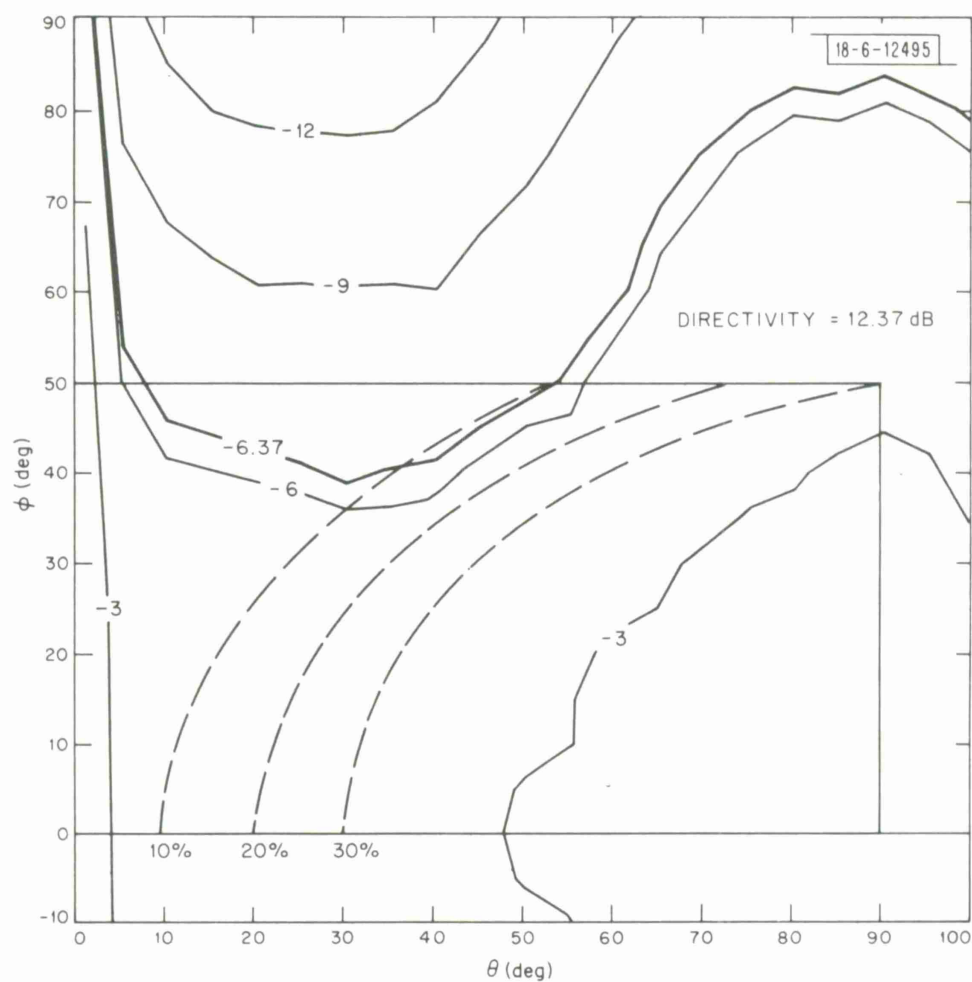


Fig. 13. Like Fig. 10, but for slots  $0.75\lambda$  long and  $0.75\lambda$  apart on  $2.80\lambda$  radius cylinder. Maximum directivity = 12.37 dB.

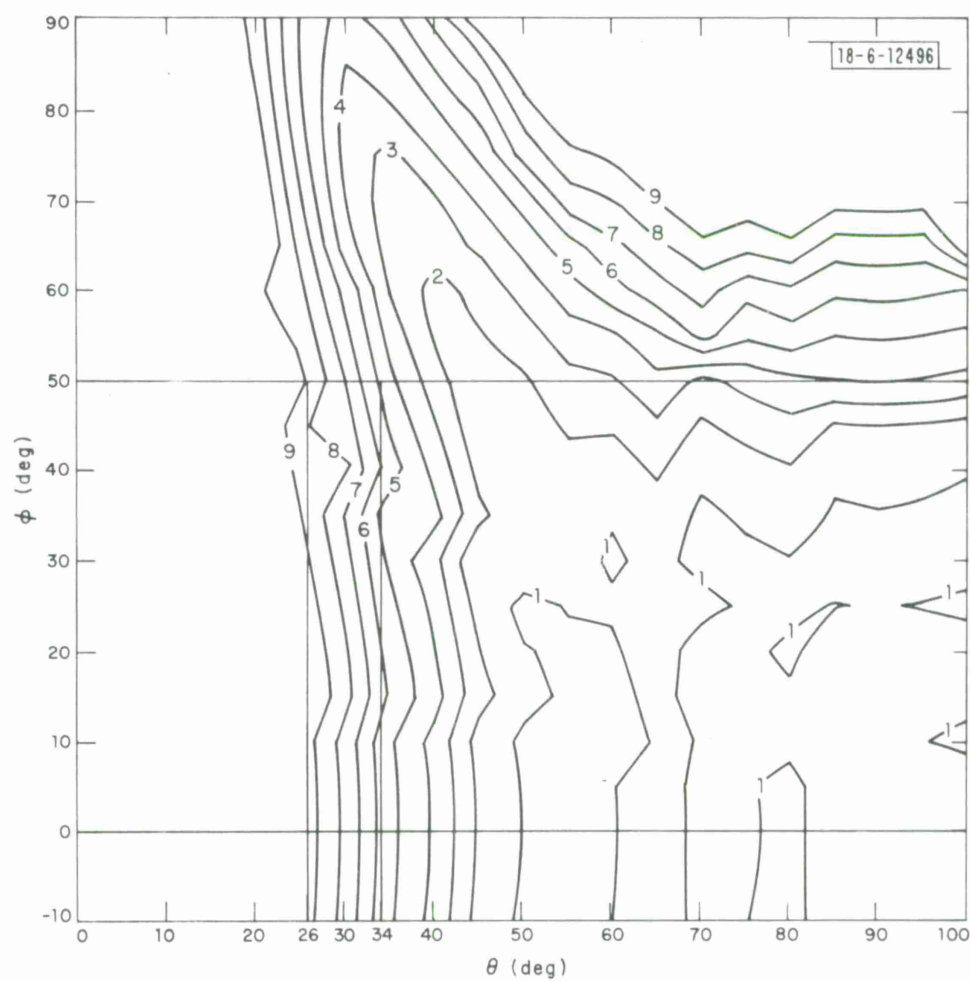


Fig. 14. Contours of axial ratios related to maximum directive gains for array of Fig. 13.

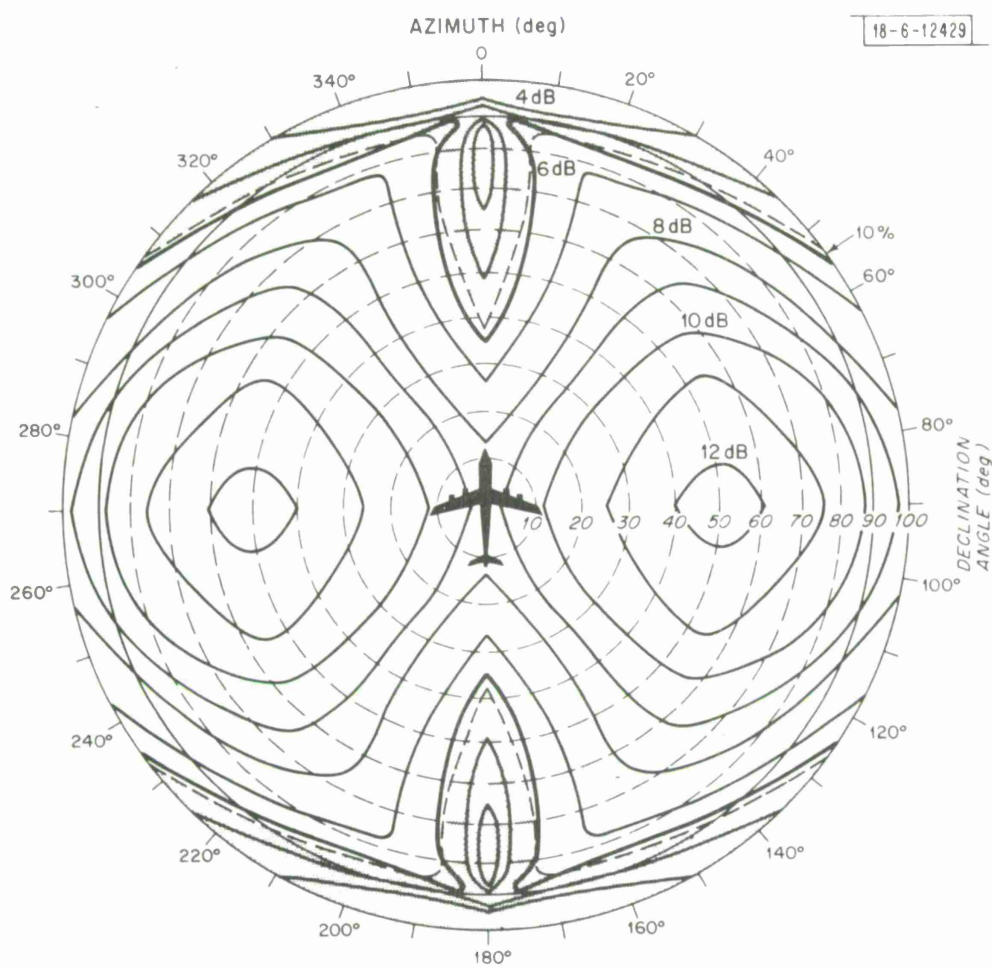


Fig. 15. Modified directive gain contours.

seen from the plot. Maximum gain occurs  $90^\circ$  away from the aircraft's heading and  $50^\circ$  down from zenith. Below horizon coverage is shown down to  $100^\circ$  from zenith. The concentric circles are at  $10^\circ$  intervals from zenith and the scale is such that areas on the polar plot are proportional to corresponding areas on a sphere. This is accomplished by setting the elemental polar area ( $\rho \, d\rho \, d\phi$ ) equal to the elemental area of a unit sphere ( $\sin \theta \, d\theta \, d\phi$ ) and solving for the polar coordinate ( $\rho$ ) in terms of the spherical coordinate ( $\theta$ ). Thus,

$$\rho = \sqrt{2(1 - \cos \theta)} \quad (13)$$

establishes the desired relationship between the radii of the concentric circles, on Fig. 15, and the corresponding angles which were taken at  $10^\circ$  intervals from zenith to  $10^\circ$  below the horizon. This method avoids the compression of data near the outer edge which orthographic projection would give and permits an estimate of the actual areas of interest on a sphere.

Since the areas of most concern are those fore and aft, the 10 percent theoretical curve of Fig. 10 has been superimposed on the contours of Fig. 15. This is the dashed curve between the 5 dB and 7 dB contours; it most nearly corresponds to the 6 dB contour. This shows that with the worst case considered here ( $0.75\lambda$  slots,  $0.75\lambda$  apart) coverage is close to 90 percent of the desired area even including the effect of the high axial ratios in the fore and aft regions.

## VI. MODIFICATIONS

Before going into the additions required to improve the performance in the fore and aft directions, modifications to the basic system will be discussed. These are concerned mainly with the excitation of the individual antenna elements. More investigation is required to optimize the excitation, perhaps by changing the magnitude as well as the phase of the excitation voltages. Thus far, only the phase has been investigated and this has been limited to identical phasing (at any one time) for both the axial and circumferential slot arrays which results, in general, in the beams being tilted differently. That is, the axially polarized beam does not point in the same direction as the circumferentially polarized beam except for the in-phase case when the beam is normal to the surface containing the elements. Of course, the difference in pointing direction is small for the smaller angles off the normal and increases as the beam tilt is increased.

This problem is compounded by the fact that the phasing requirements are different for the transmit and receive frequencies. One modification that should definitely be considered is the possibility of using separate phasing devices for the two frequencies. This might be accomplished by dividing the band-pass filters, which perform the duplexing function, into two parts: one near the antenna elements and one near the transmitter and receiver. At the antenna, each band-pass filter need only provide relatively low isolation (about 20 dB) between the two frequencies and the remainder of the required

isolation would be provided by the units near the transmitter and receiver. Thus, there would be enough isolation to permit the use of a variable phasing unit on each side. Figure 16 is a block diagram illustrating the system.

One of the problems discussed in the previous section (V) arises because the slots should be longer than  $\lambda/2$  for impedance reasons, but closer together than  $\lambda/2$  for directive-gain and axial-ratio reasons. Radiation characteristics were presented for an arrangement of crossed slots as shown in Fig. 17(a). Crossed slots are shown as orthogonal lines and the square around each set represents the cavity. Figure 17(b) shows a more compact arrangement of the same size slots and cavities. This arrangement permits axial and circumferential slot elements to be placed much closer together, and more desirable radiation characteristics should be the result. However, the rows are not identical, a necessary condition for the present computer program.<sup>5</sup> A modification of the program will be undertaken as a continuation of the VHF antenna investigation.

Other modifications to the basic system will become apparent as the research progresses. One obvious need is for coverage in the forward and aft areas of the aircraft. This requires additional antenna elements to fill in the nulls left by the basic system. A possible solution would be to put a plate antenna<sup>6</sup> on the forward surface of the aircraft and another on the aft surface.

In its simplest form, a plate antenna is a square conducting sheet spaced a small part of a wavelength away from a ground plane. It is fed across the

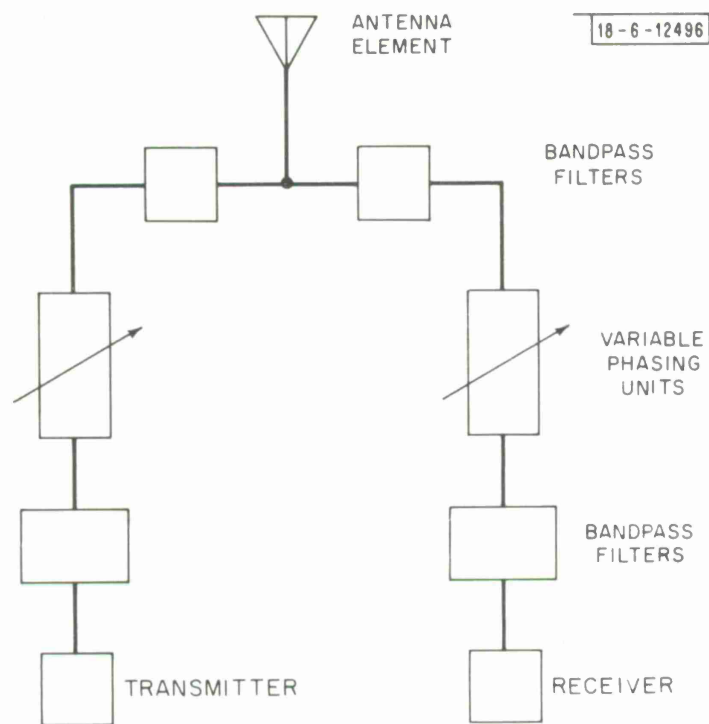


Fig. 16. Block diagram of separate phasing units for transmit and receive frequencies.



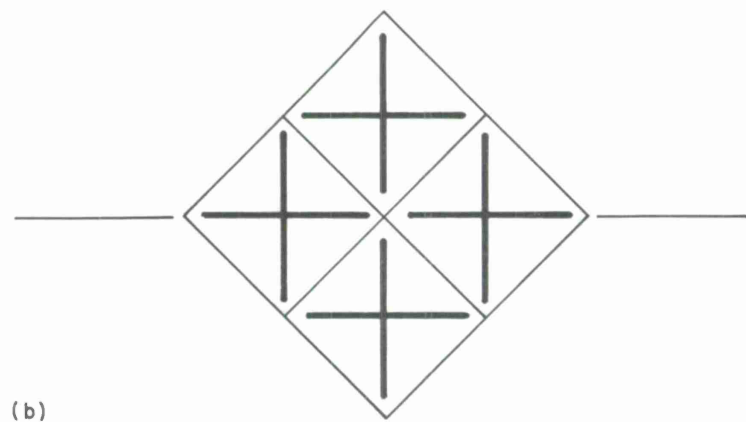
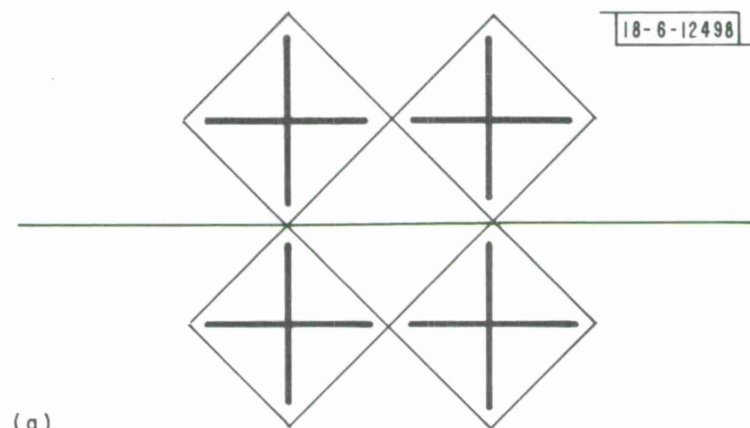


Fig. 17. Alternative crossed-slot array arrangements.

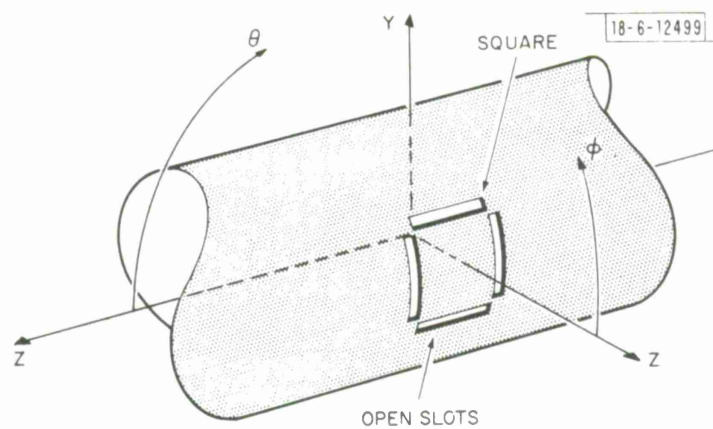


Fig. 18. Square-plate antenna on cylinder.

gap between it and the ground plane either across flats or across corners with voltages which are equal in magnitude and opposite in phase. By using two orthogonal feeds with a quadrature phase relationship, circularly polarized radiation is produced with maximum field normal to the plate. A plate  $\lambda/2$  square has a directivity of about 9 dB and a half-power beamwidth of about  $60^\circ$ . Therefore it can provide coverage with  $> 6$  dB directive gain over a cone of about  $30^\circ$  half angle. Over the area of coverage, the axial ratio is less than 3 dB.

Analysis of the square plate antenna is similar to that of the crossed slots. Figure 18 shows a pair of axial slots and a pair of circumferential slots, with all slots of equal length, arrayed to form a square on the surface of an infinitely long conducting cylinder. For each pair of slots, the directive gain (D) and phase ( $\beta$ ) are computed as they were for the crossed slots. These values are used in Eqs. (8) through (10) to get the radiation characteristics cited previously for the  $\lambda/2$  square-plate antenna.

For VHF operation, the plate would be about 20 inches square. It can be used as a so-called "paste-on" antenna conforming to the surface of the aircraft and separated from it by a sheet of dielectric material. This antenna element could be considered as an addition to the basic system described in this report.

## VII. CONCLUSION

Preliminary research of a VHF antenna system indicates that it should

have improved performance over those presently used on aircraft for satellite communications. The basic system consists of two array antennas strategically located on the aircraft. Each array consists of four crossed-slot antenna elements. By the use of variable phasing devices, a circularly polarized beam is pointed toward the communications satellite. The coverage goal is the hemisphere above the aircraft and  $10^\circ$  below the horizon with a directive gain of at least 6 dB and axial ratios less than 6 dB. Computed data show the basic system should attain about 90 percent of the goal. Only the usual fore and aft problem areas would not be covered within the specified limits. Addition of two square plate antenna elements to the basis system can fill in these problem areas and complete the coverage.

## REFERENCES

1. "IEEE Standard Definitions of Terms for ANTENNAS," No. 145 (March 1969).
2. C.A. Lindberg, "A Shallow-Cavity UHF Crossed-Slot Antenna," Technical Report 446, Lincoln Laboratory, M.I.T. (8 March 1968), DDC AD-672763.
3. R. N. Assaly, M.E. Devane, B.F. LaPage, M.L. Rosenthal and A. Sotiropoulos, "LES-6 Antenna System," Technical Report 465, Lincoln Laboratory, M.I.T. (10 March 1969), DDC AD-693197.
4. M.L. Rosenthal, M.E. Devane and B.F. LaPage, "VHF Antenna Systems for Spin-Stabilized Satellites," IEEE Trans. Ant. and Prop., AP-17, No. 4, pp. 443-451 (July 1969), DDC AD-696883.
5. L.J. Ricardi, "Directivity of an Array of Slots on the Surface of a Cylinder," Technical Note 1966-52, Lincoln Laboratory, M.I.T. (10 October 1966), DDC AD-641959; also Electron. Eng. 39, p. 578 (1967), DDC AD-668239.
6. L.J. Ricardi and M.L. Rosenthal, "Plate Antenna with Polarization Adjustment," U.S. Patent Office, 3, 478, 362 (11 November 1969).

DOCUMENT CONTROL DATA - R&D

(Security classification of title, body of abstract and indexing annotation must be entered when the overall report is classified)

1. ORIGINATING ACTIVITY (Corporate author)  Lincoln Laboratory, M. I. T.		2a. REPORT SECURITY CLASSIFICATION Unclassified													
		2b. GROUP None													
3. REPORT TITLE  VHF Antenna System for Aircraft															
4. DESCRIPTIVE NOTES (Type of report and inclusive dates) Technical Note															
5. AUTHOR(S) (Last name, first name, initial)  Rosenthal, Milton L.															
6. REPORT DATE 12 March 1970		7a. TOTAL NO. OF PAGES 44	7b. NO. OF REFS 6												
8a. CONTRACT OR GRANT NO. AF 19 (628)-5167		9a. ORIGINATOR'S REPORT NUMBER(S) Technical Note 1970-8													
b. PROJECT NO. 649L		9b. OTHER REPORT NO(S) (Any other numbers that may be assigned this report)													
c.		ESD-TR-70-53													
d.															
10. AVAILABILITY/LIMITATION NOTICES  This document has been approved for public release and sale; its distribution is unlimited.															
11. SUPPLEMENTARY NOTES  None		12. SPONSORING MILITARY ACTIVITY  Air Force Systems Command, USAF													
13. ABSTRACT  <p>Presented are the initial results of a theoretical investigation of crossed-slot antenna elements arrayed on an aircraft to provide communications with satellites in the 225 to 400 MHz frequency range. Calculations indicate that two four-element array antennas can approximate the desired performance of covering the hemisphere above the aircraft with more than 6 dB directive gain. Including the polarization loss between the elliptically polarized aircraft antenna and the circularly polarized satellite antenna, coverage is provided over about 90 percent of the desired area.</p>															
14. KEY WORDS															
<table><tr><td>crossed-slot antenna</td><td>VHF antenna</td><td>circular polarization</td></tr><tr><td>array antenna</td><td>satellite-to-air communications</td><td>directive gain</td></tr><tr><td>aircraft antenna</td><td>airborne terminal</td><td>beam steering</td></tr><tr><td>satellite antenna</td><td>hemispheric coverage</td><td></td></tr></table>				crossed-slot antenna	VHF antenna	circular polarization	array antenna	satellite-to-air communications	directive gain	aircraft antenna	airborne terminal	beam steering	satellite antenna	hemispheric coverage	
crossed-slot antenna	VHF antenna	circular polarization													
array antenna	satellite-to-air communications	directive gain													
aircraft antenna	airborne terminal	beam steering													
satellite antenna	hemispheric coverage														



